features. It appears that $EpCAM^+$ cells, but not $EpCAM^-$ cells, have self-renewal and differentiation capabilities with the ability to form colonies from a single cell, and produce both $EpCAM^+$ and $EpCAM^-$ cells.

It has been previously demonstrated that stem/progenitor cells and cancer stem/progenitor cells can form spheroids *in vitro* in a non-attached condition [36, 37]. Consistently, $EpCAM^+$ cells could form spheroids efficiently, reaching to about 150~200 μm in diameter after 14 days culture (Fig 4A-B). Interestingly, all cells in a spheroid were $EpCAM^+$ while AFP expression was relatively heterogeneous (Fig 4C-D, Suppl Movie 1). Rarely, a few spheroids derived from an $EpCAM^-$ cell fraction were positive for EpCAM (data not shown), suggesting that these spheroids were derived from contaminated residual $EpCAM^+$ cells by FACS sorting. All spheroid cells maintained EpCAM expression while half of the attached cells lost EpCAM expression when the $EpCAM^+$ fraction was cultured for 14 days (Fig 4E). Most spheroid cells also abundantly expressed PCNA, implying active cell proliferation (Fig 4F and Suppl Movie 2). Thus, a subset of $EpCAM^+$ cells, but not $EpCAM^-$ cells, can form spheroids.

$EpCAM^+$ HCC cells as tumor initiating cells

$EpCAM^+$ HCC cells, but not $EpCAM^-$ HCC cells, could efficiently initiate invasive tumors in NOD/SCID mice (Fig 5). For example, 10,000 $EpCAM^+$ HuH1 cells produced large hypervascular tumors in 100% of mice whereas $EpCAM^-$ cell fractions produced only small and pale looking tumors in 30% of mice 4 weeks after injection (Fig 5A, Suppl Fig 3A). Similar results were obtained with HuH7 cells (Suppl Fig 3B-D). As little as 200 $EpCAM^+$ cells could initiate tumors in 8 of 10 injected mice, whereas 200 $EpCAM^-$ cells produced only one tumor among 10 injected mice at 6 weeks after transplantation, and the tumor sizes were much larger in the $EpCAM^+$ cells than the $EpCAM^-$ cells (Fig 5B and Suppl Fig 3E). $EpCAM^+$ cells produced tumors with a mixture of both $EpCAM^+$ and $EpCAM^-$ cells in xenografts, and these cells invaded in the capsule and muscles of the leg adjacent to the tumor (Fig 5C). $EpCAM^+$ cells derived from tumors again maintained their tumor initiating capacity, tumor morphology and invasive ability in an *in vivo* serial transplantation experiment (Fig 5D). Occasionally, $EpCAM^-$ cell fraction produced a few small tumors that always contain a mixture of $EpCAM^+$ and $EpCAM^-$ cells (data not shown), indicating that the tumor-initiating ability is contributed by the contaminated $EpCAM^+$ cells from FACS sorting.

To further validate whether $EpCAM^+$ HCC cells were tumor initiating cells, we isolated $EpCAM^+$ HCC cells from two cases of AFP^+ (>600 ng/ml serum AFP) HCC clinical specimens using MACS. Consistently, 1×10^4 $EpCAM^+$ cells could induce tumors in NOD/SCID mice, but up to 1×10^6 $EpCAM^-$ cells failed to do so (Table 1). In addition, similar to HCC cell lines, fresh $EpCAM^+$ tumor cells from two clinical HCC specimens were more efficient in forming spheroids *in vitro* than $EpCAM^-$ cells (Suppl Fig 4).

FACS analysis results indicate that a majority of $EpCAM^+$ cells express CD133 in HuH7 cells but not in HuH1 cells (Fig 2B), which prompted us to compare the tumorigenic capacity of $EpCAM^+$ and $CD133^+$ cells in these cell lines. Noticeably, $EpCAM^+$ HuH1 cells showed marked tumor initiating capacity compared with $CD133^+$ HuH1 cells (Fig 5E-F), whereas $EpCAM^+$ and $CD133^+$ cells had the similar tumorigenic ability in HuH7 cells (data not shown).

GSK-3β inhibition augments $EpCAM^+$ HCC cells

To determine the role of Wnt/β-catenin signaling [28] in $EpCAM^+$ HCC cells (Fig 1B), we first treated HuH1, HuH7, and HLF cells with a GSK-3β inhibitor BIO (Fig 6A), which activates Wnt/β-catenin signaling (Fig 6B) and maintains undifferentiation of embryonic stem cells [38]. BIO increased the $EpCAM^+$ cell population in HuH1 and HuH7 cells when compared to the control methylated BIO (MeBIO) (Fig 6A). In contrast, BIO had no effect on the $CD90^+$ cell

population that is more tumorigenic than the CD90$^-$ cell population in HLF (Fig 6A and data not shown). Enrichment of EpCAM$^+$ cells was further provoked by the treatment of Wnt10B-conditioned media in HuH7 cells (Fig 6C) [34]. BIO induced morphological alteration of HuH7 cells as most cells became small and round when compared to MeBIO and suppressed EpCAM$^-$ AFP$^-$ cell population (Fig 6D). Moreover, BIO induced *TACSTD1, MYC*, and *hTERT* expression and spheroid formation (Fig 6E-F).

EpCAM blockage by RNA interference

One of the hallmarks of CSCs is its resistance to conventional chemotherapeutic agents resulting in tumor relapse and thus targeting CSCs is critical to achieve successful tumor remission. Consistently, 5-FU could increase the EpCAM$^+$ population and spheroid formation of HuH1 and HuH7 cells (Fig 7A-B) (data not shown), suggesting a differential sensitivity of EpCAM$^+$ and EpCAM$^-$ HCC cells to 5-FU. In contrast, EpCAM blockage via RNA interference dramatically decreased the population of EpCAM$^+$ cells (Fig 7C), and significantly inhibited cellular invasion, spheroid formation and tumorigenicity of HuH1 cells (Fig 7D-F). Thus, EpCAM may serve as a molecular target to eliminate HCC cells with stem/progenitor cell features.

DISCUSSION

The cellular origin of HCC is currently in debate. In this study, we found that EpCAM can serve as a marker to enrich HCC cells with tumor initiating ability and with some stem/progenitor cell traits. EpCAM is expressed in many human cancers with an epithelium origin 39. During embryogenesis, EpCAM is expressed in fertilized oocytes, embryonic stem cells and embryoid bodies, suggesting its role in early stage embryogenesis 40. Furthermore, a recent paper indicates that EpCAM is expressed in colonic and breast CSCs 41. Taken together, these data suggest a critical role of EpCAM in CSCs as well as embryonic and somatic stem cells. Consistently, we found that EpCAM expression is regulated by Wnt/β-catenin signaling [29] and tumorigenic and highly invasive HpSC-HCC is orchestrated by a subset of cells expressing EpCAM and AFP with stem cell-like features and self-renewal and differentiation capabilities regulated by Wnt/β-catenin signaling (this study). Thus, EpCAM may be a common gene expressed in undifferentiated normal and HCC with activated Wnt/β-catenin signaling. It may act as a downstream molecule to maintain HCC "stemness" and serve as a good marker for HCC initiating cells.

CD133 or CD90 have been used to identify potential hepatic CSCs [35, 42]. CD133 is expressed in normal and malignant stem cells of the neural, hematopoietic, epithelial, hepatic and endothelial lineages [23, 43, 44], suggesting that CD133 is also a common marker to detect normal and CSCs. Captivatingly, EpCAM expression overlaps with CD133 expression in normal human colon tissues and colorectal cancer tissues, yet CD133$^+$ and CD133$^-$ cells are equally tumorigenic 45. Similarly, we found that EpCAM$^+$ and EpCAM$^-$ HuH1 cells equally expressed CD133 but only EpCAM$^+$ cells developed large hypervascular tumors. Our data suggest that EpCAM may be a better marker than CD133 to enrich HCC tumor initiating cells from AFP$^+$ tumors. We also found that CD90 expression was limited to HCC cell lines that are EpCAM$^-$ AFP$^-$, and Wnt/β-catenin signaling had little effect on CD90$^+$ cell enrichment. These results suggest that the expression patterns of various stem cell markers in tumor initiating cells with stem/progenitor cell features may be different in each HCC subtype, possibly due to the heterogeneity of activated signaling pathways in normal stem/progenitor cells where these tumor initiating cells may originate. Therefore, it would be useful to comprehensively investigate the expression patterns of stem cell markers to characterize the population of CSC that may correlate with the activation of their distinct molecular pathways.

CSCs may be more resistant to chemotherapeutic agents than differentiated tumor cells possibly due to an increased expression of ATP-binding cassette transporters and anti-apoptotic proteins [4]. Thus, development of an effective strategy to target CSC pools together with conventional chemotherapies is essential to eradicate a tumor mass [14]. By blocking the programs that activate self-renewal and/or inhibit asymmetric division, CSC features could be "destemmed" [46, 47]. Consistently, EpCAM blockage could inhibit cellular invasion and tumorigenicity of $EpCAM^+$ HCC cells, revealing the feasibility of targeting a CSC marker to "destem" CSC features. EpCAM may induce c-Myc [48], a common molecular node activated in HpSC-HCC [27]. c-Myc, together with Oct3/4, Sox2, and Klf4, can induce pluripotent stem cells from adult fibroblasts [49]. It is possible that EpCAM blockage to inhibit hepatic CSCs may result in a suppression of c-Myc signaling. Encouragingly, EpCAM-specific antibodies are currently in phase II clinical trials [50].

Furthermore, a recent study indicates that $EpCAM^+$ circulating tumor cells identified by a unique microfluidic platform can be used to monitor patient outcomes undergoing systemic treatment [51]. Therefore, it may be useful to combine EpCAM antibodies with conventional chemotherapy to target both CSCs and non-CSCs for the treatment of HCC.

Supplementary Material

Refer to Web version on PubMed Central for supplementary material.

Acknowledgments

We thank Drs. Curtis Harris and Sharon Pine for critical readings of the manuscript; Ms. Barbara Taylor and Dr. Susan Garfield for technical assistance; Drs. Ali Brivanlou (Rockefeller University), Steve Strom (University of Pittsburgh), and Bert Vogelstein (Johns Hopkins University) for generously providing their research materials.

Grant Support: This work was supported in part by the Intramural Research Program of the Center for Cancer Research, the US National Cancer Institute. H.-L.J, Q.-H.Y., L.-X.Q, and Z.-Y.T. were supported by the research grants from the China National Natural Science Foundation for Distinguished Young Scholars (30325041) and the China National "863" R&D High-Tech Key Project (2002BA711A02-4). L.M.R. was supported by a sponsored research grant from Vesta Therapeutics (Research Triangle Park, NC), NIH grants (RO1 AA014243 , RO1 IP30-DK065933), and a U.S. Department of Energy grant (DE-FG02-02ER-63477). Sponsors have no role in the study design, data collection, analysis and interpretation.

References

1. Fialkow PJ. Clonal origin of human tumors. Biochim Biophys Acta 1976;458:283–321. [PubMed: 1067873]
2. Heppner GH. Tumor heterogeneity. Cancer Res 1984;44:2259–2265. [PubMed: 6372991]
3. Hanahan D, Weinberg RA. The hallmarks of cancer. Cell 2000;100:57–70. [PubMed: 10647931]
4. Jordan CT, Guzman ML, Noble M. Cancer stem cells. N Engl J Med 2006;355:1253–1261. [PubMed: 16990388]
5. Clarke MF, Dick JE, Dirks PB, et al. Cancer stem cells--perspectives on current status and future directions: AACR Workshop on cancer stem cells. Cancer Res 2006;66:9339–9344. [PubMed: 16990346]
6. Potter VR. Phenotypic diversity in experimental hepatomas: the concept of partially blocked ontogeny. The 10th Walter Hubert Lecture. Br J Cancer 1978;38:1–23. [PubMed: 356869]
7. Sell S. Cellular origin of cancer: dedifferentiation or stem cell maturation arrest? Environ Health Perspect 1993;101(Suppl 5):15–26. [PubMed: 7516873]
8. Wicha MS, Liu S, Dontu G. Cancer stem cells: an old idea--a paradigm shift. Cancer Res 2006;66:1883–1890. [PubMed: 16488983]
9. Al Hajj M, Wicha MS, Benito-Hernandez A, et al. Prospective identification of tumorigenic breast cancer cells. Proc Natl Acad Sci U S A 2003;100:3983–3988. [PubMed: 12629218]

10. Singh SK, Hawkins C, Clarke ID, et al. Identification of human brain tumour initiating cells. Nature 2004;432:396–401. [PubMed: 15549107]
11. Bonnet D, Dick JE. Human acute myeloid leukemia is organized as a hierarchy that originates from a primitive hematopoietic cell. Nat Med 1997;3:730–737. [PubMed: 9212098]
12. Ricci-Vitiani L, Lombardi DG, Pilozzi E, et al. Identification and expansion of human colon-cancer-initiating cells. Nature 2007;445:111–115. [PubMed: 17122771]
13. O'Brien CA, Pollett A, Gallinger S, et al. A human colon cancer cell capable of initiating tumour growth in immunodeficient mice. Nature 2007;445:106–110. [PubMed: 17122772]
14. Dean M, Fojo T, Bates S. Tumour stem cells and drug resistance. Nat Rev Cancer 2005;5:275–284. [PubMed: 15803154]
15. Rich JN. Cancer stem cells in radiation resistance. Cancer Res 2007;67:8980–8984. [PubMed: 17908997]
16. Parkin DM, Bray F, Ferlay J, et al. Global cancer statistics, 2002. CA Cancer J Clin 2005;55:74–108. [PubMed: 15761078]
17. Sell S, Pierce GB. Maturation arrest of stem cell differentiation is a common pathway for the cellular origin of teratocarcinomas and epithelial cancers. Lab Invest 1994;70:6–22. [PubMed: 8302019]
18. Thorgeirsson SS, Grisham JW. Hepatic stem cells. Semin Liver Dis 2003;23:301.
19. Thorgeirsson SS, Grisham JW. Molecular pathogenesis of human hepatocellular carcinoma. Nat Genet 2002;31:339–346. [PubMed: 12149612]
20. Lee JS, Heo J, Libbrecht L, et al. A novel prognostic subtype of human hepatocellular carcinoma derived from hepatic progenitor cells. Nat Med 2006;12:410–416. [PubMed: 16532004]
21. Sigal SH, Brill S, Fiorino AS, et al. The liver as a stem cell and lineage system. Am J Physiol 1992;263:G139–G148. [PubMed: 1325126]
22. Schmelzer E, Wauthier E, Reid LM. The Phenotypes of Pluripotent Human Hepatic Progenitors. Stem Cells 2006;24:1852–1858. [PubMed: 16627685]
23. Schmelzer E, Zhang L, Bruce A, et al. Human hepatic stem cells from fetal and postnatal donors. J Exp Med 2007;204:1973–1987. [PubMed: 17664288]
24. Dan YY, Riehle KJ, Lazaro C, et al. Isolation of multipotent progenitor cells from human fetal liver capable of differentiating into liver and mesenchymal lineages. Proc Natl Acad Sci U S A 2006;103:9912–9917. [PubMed: 16782807]
25. Zaret KS. Regulatory phases of early liver development: paradigms of organogenesis. Nat Rev Genet 2002;3:499–512. [PubMed: 12094228]
26. Shafritz DA, Oertel M, Menthena A, et al. Liver stem cells and prospects for liver reconstitution by transplanted cells. Hepatology 2006;43:S89–S98. [PubMed: 16447292]
27. Yamashita T, Forgues M, Wang W, et al. EpCAM and alpha-fetoprotein expression defines novel prognostic subtypes of hepatocellular carcinoma. Cancer Res 2008;68:1451–1461. [PubMed: 18316609]
28. Reya T, Clevers H. Wnt signalling in stem cells and cancer. Nature 2005;434:843–850. [PubMed: 15829953]
29. Yamashita T, Budhu A, Forgues M, et al. Activation of hepatic stem cell marker EpCAM by Wnt-ß-catenin signaling in hepatocellular carcinoma. Cancer Research 2007;67:10831–10839. [PubMed: 18006828]
30. Budhu A, Forgues M, Ye QH, et al. Prediction of venous metastases, recurrence and prognosis in hepatocellular carcinoma based on a unique immune response signature of the liver microenvironment. Cancer Cell 2006;10:99–111. [PubMed: 16904609]
31. Ye QH, Qin LX, Forgues M, et al. Predicting hepatitis B virus-positive metastatic hepatocellular carcinomas using gene expression profiling and supervised machine learning. Nat Med 2003;9:416–423. [PubMed: 12640447]
32. Wu CG, Forgues M, Siddique S, et al. SAGE transcript profiles of normal primary human hepatocytes expressing oncogenic hepatitis B virus X protein. FASEB J 2002;16:1665–1667. [PubMed: 12207007]

33. Kubota H, Reid LM. Clonogenic hepatoblasts, common precursors for hepatocytic and biliary lineages, are lacking classical major histocompatibility complex class I antigen. Proc Natl Acad Sci U S A 2000;97:12132–12137. [PubMed: 11050242]
34. Yoshikawa H, Matsubara K, Zhou X, et al. WNT10B Functional Dualism: beta-Catenin/Tcf-dependent Growth Promotion or Independent Suppression with Deregulated Expression in Cancer. Mol Biol Cell 2007;18:4292–4303. [PubMed: 17761539]
35. Yang ZF, Ho DW, Ng MN, et al. Significance of CD90(+) Cancer Stem Cells in Human Liver Cancer. Cancer Cell 2008;13:153–166. [PubMed: 18242515]
36. Dontu G, Abdallah WM, Foley JM, et al. In vitro propagation and transcriptional profiling of human mammary stem/progenitor cells. Genes Dev 2003;17:1253–1270. [PubMed: 12756227]
37. Fang D, Nguyen TK, Leishear K, et al. A tumorigenic subpopulation with stem cell properties in melanomas. Cancer Res 2005;65:9328–9337. [PubMed: 16230395]
38. Sato N, Meijer L, Skaltsounis L, et al. Maintenance of pluripotency in human and mouse embryonic stem cells through activation of Wnt signaling by a pharmacological GSK-3-specific inhibitor. Nat Med 2004;10:55–63. [PubMed: 14702635]
39. Balzar M, Winter MJ, de Boer CJ, et al. The biology of the 17-1A antigen (Ep-CAM). J Mol Med 1999;77:699–712. [PubMed: 10606205]
40. Trzpis M, McLaughlin PM, de Leij LM, et al. Epithelial cell adhesion molecule: more than a carcinoma marker and adhesion molecule. Am J Pathol 2007;171:386–395. [PubMed: 17600130]
41. Dalerba P, Dylla SJ, Park IK, et al. Phenotypic characterization of human colorectal cancer stem cells. Proc Natl Acad Sci U S A 2007;104:10158–10163. [PubMed: 17548814]
42. Ma S, Chan KW, Hu L, et al. Identification and characterization of tumorigenic liver cancer stem/progenitor cells. Gastroenterology 2007;132:2542–2556. [PubMed: 17570225]
43. Yin AH, Miraglia S, Zanjani ED, et al. AC133, a novel marker for human hematopoietic stem and progenitor cells. Blood 1997;90:5002–5012. [PubMed: 9389720]
44. Fargeas CA, Corbeil D, Huttner WB. AC133 antigen, CD133, prominin-1, prominin-2, etc.: prominin family gene products in need of a rational nomenclature. Stem Cells 2003;21:506–508. [PubMed: 12832703]
45. Shmelkov SV, Butler JM, Hooper AT, et al. CD133 expression is not restricted to stem cells, and both CD133+ and CD133− metastatic colon cancer cells initiate tumors. J Clin Invest 2008;118:2111–2120. [PubMed: 18497886]
46. Hill RP, Perris R. "Destemming" cancer stem cells. J Natl Cancer Inst 2007;99:1435–1440. [PubMed: 17895479]
47. Piccirillo SG, Reynolds BA, Zanetti N, et al. Bone morphogenetic proteins inhibit the tumorigenic potential of human brain tumour-initiating cells. Nature 2006;444:761–765. [PubMed: 17151667]
48. Munz M, Kieu C, Mack B, et al. The carcinoma-associated antigen EpCAM upregulates c-myc and induces cell proliferation. Oncogene 2004;23:5748–5758. [PubMed: 15195135]
49. Takahashi K, Tanabe K, Ohnuki M, et al. Induction of pluripotent stem cells from adult human fibroblasts by defined factors. Cell 2007;131:861–872. [PubMed: 18035408]
50. Chaudry MA, Sales K, Ruf P, et al. EpCAM an immunotherapeutic target for gastrointestinal malignancy: current experience and future challenges. Br J Cancer 2007;96:1013–1019. [PubMed: 17325709]
51. Nagrath S, Sequist LV, Maheswaran S, et al. Isolation of rare circulating tumour cells in cancer patients by microchip technology. Nature 2007;450:1235–1241. [PubMed: 18097410]

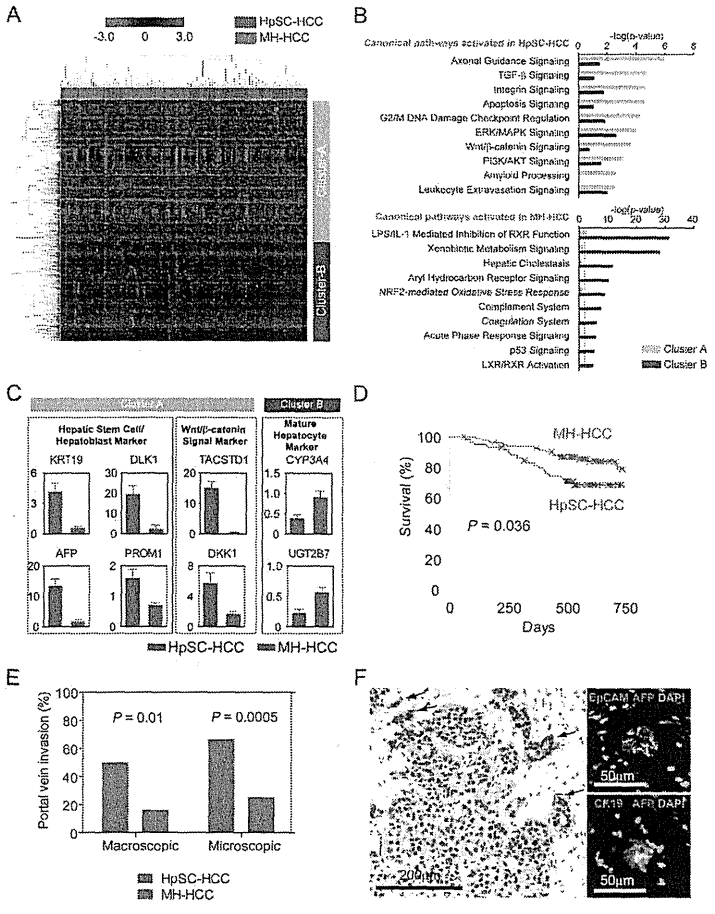

Figure 1.

HpSC-HCC represents a subset of invasive HCCs with cancer stem cells (CSC) Features. (A) Hierarchical cluster analysis based on 793 HpSC-HCC-coregulated genes in 156 HCC cases. Each cell in the matrix represents the expression level of a gene in an individual sample. Red and green cells depict high and low expression levels, respectively, as indicated by the scale bar. (B) Pathway analysis of HpSC-HCC-coregulated genes. The top ten canonical signaling pathways activated in cluster-A (upper panel) or cluster-B (lower panel) with statistical significance ($P < 0.01$) are shown. (C) Expression patterns of well-known HpSC and MH markers in each HCC subtype as analyzed by microarray. (D) Kaplan-Meier survival analysis of the cases used for array analysis. (E) Frequency of macroscopic and microscopic portal vein invasion in HpSC-HCC and MH-HCC used for IHC. (F) Representative images of EpCAM, AFP, and CK19 staining in HpSC-HCC samples analyzed by IHC and IF. EpCAM staining illustrates heterogeneous expression of EpCAM in HpSC-HCC (left panel). $EpCAM^+$ cells were disseminated in the invasive border (left panel black arrows) with expression of AFP (right top panel) and CK19 (right bottom panel).

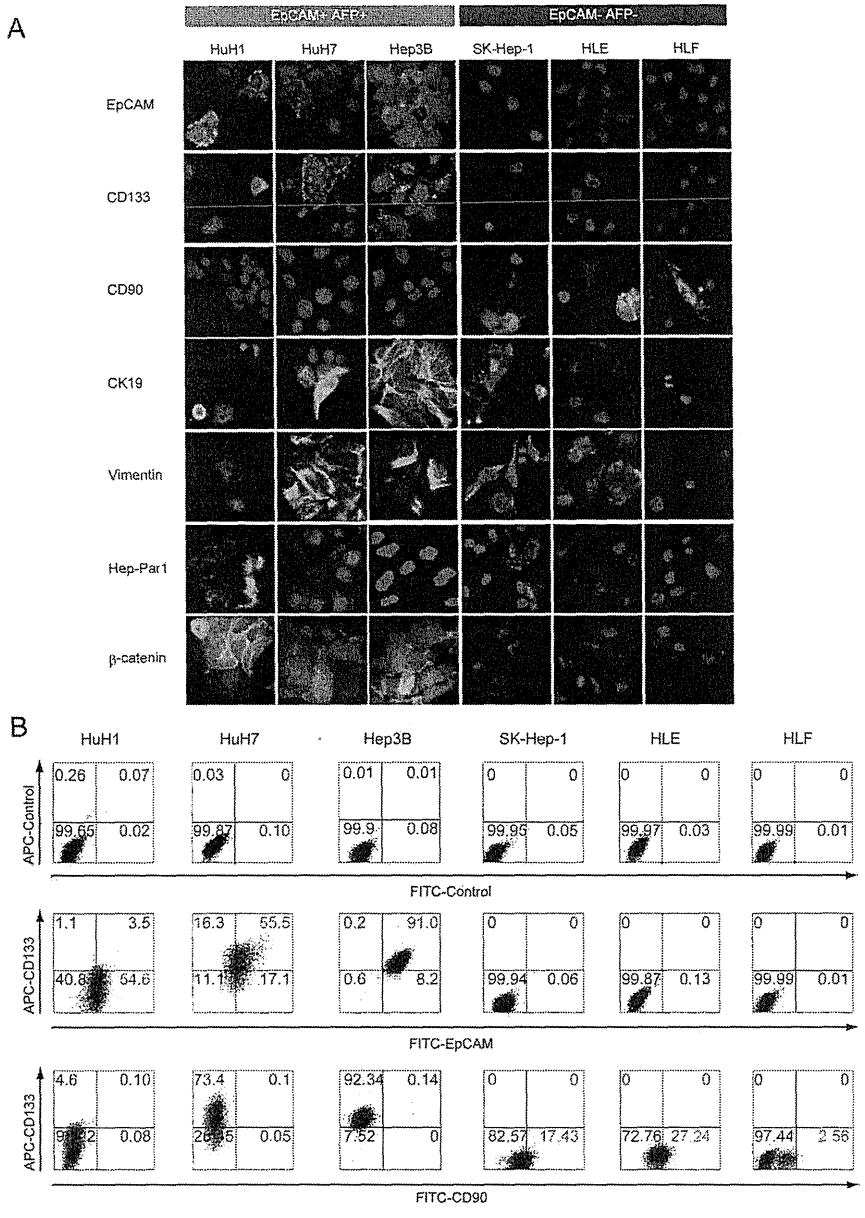

Figure 2.

Characterization of hepatic stem cell marker expression in HCC cell lines. (A) IF analysis of six HCC cell lines (EpCAM$^+$ AFP$^+$ cell lines; HuH1, HuH7, and Hep3B, EpCAM$^-$ AFP$^-$ cell lines; SK-Hep-1, HLE, and HLF) stained with anti-EpCAM, anti-CD133, anti-CD90, anti-CK19, anti-Vimentin, anti-Hep-Par1, and anti-β-catenin antibodies. (B) FACS analysis of six HCC cell lines stained with anti-EpCAM, anti-CD133, and anti-CD90 antibodies.

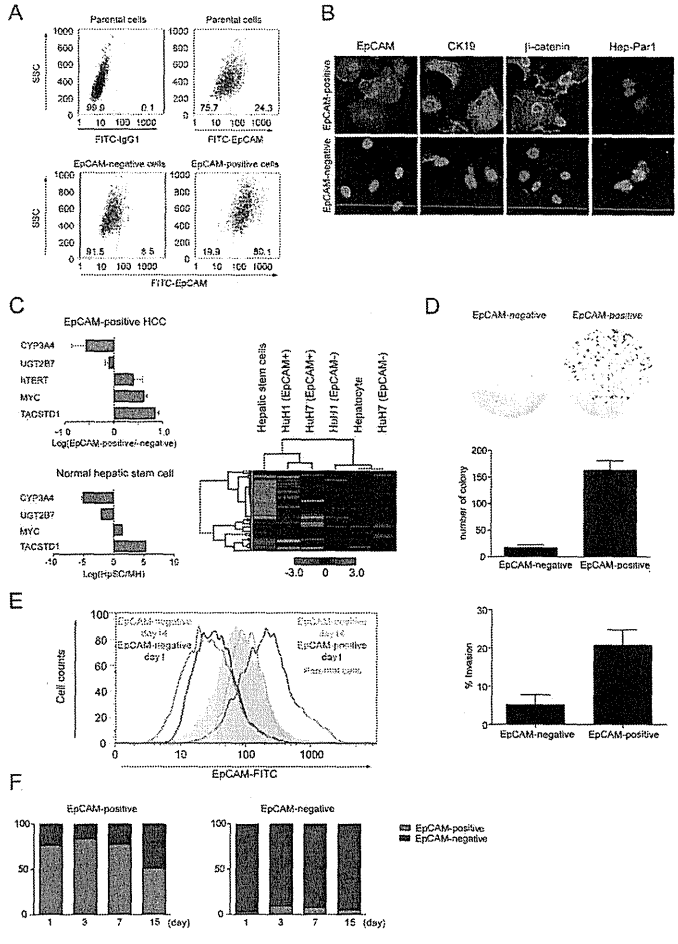

Figure 3.

Characterization of EpCAM$^+$ and EpCAM$^-$ cells in HuH7 cells. (A) FACS analysis of EpCAM$^+$ and EpCAM$^-$ cells day 1 after cell sorting. (B) IF analysis of cells stained with anti-EpCAM, anti-AFP, anti-CK19, or anti-β-catenin antibodies. (C) qRT-PCR analysis of EpCAM$^+$ and EpCAM$^-$ HuH7 cells (left upper panel) or hepatic stem cells (HpSC) and mature hepatocytes (MH) (left lower panel). Experiments were performed in triplicate. Hierarchical cluster analysis of HpSC, MH, EpCAM$^+$ and EpCAM$^-$ HCC cells using a panel of genes expressed in human embryonic stem cells (right panel). Gene expression was measured in quadruplicate. (D) Representative photographs of the plates containing colonies derived from 2,000 EpCAM$^+$ or EpCAM$^-$ HuH7 cells (upper panel). Colony formation experiments were performed in triplicate (mean ± SD) (middle panel). Cell invasiveness of EpCAM$^+$ and EpCAM$^-$ cells using the Matrigel invasion assay (lower panel). (E) Flow cytometer analysis of EpCAM$^+$ and EpCAM$^-$ HuH7 cells stained with anti-EpCAM at day 1 and 14 after cell sorting. (F) Percent of sorted EpCAM$^+$ and EpCAM$^-$ cells after culturing with various times as analyzed by IF. Numbers of EpCAM$^+$ and EpCAM$^-$ cells were counted in three independent areas of Chamber Slides at day 1, 3, 7, and 15 after cell sorting. The average percentages of EpCAM$^+$ or $^-$ cells are depicted as red or blue, respectively.

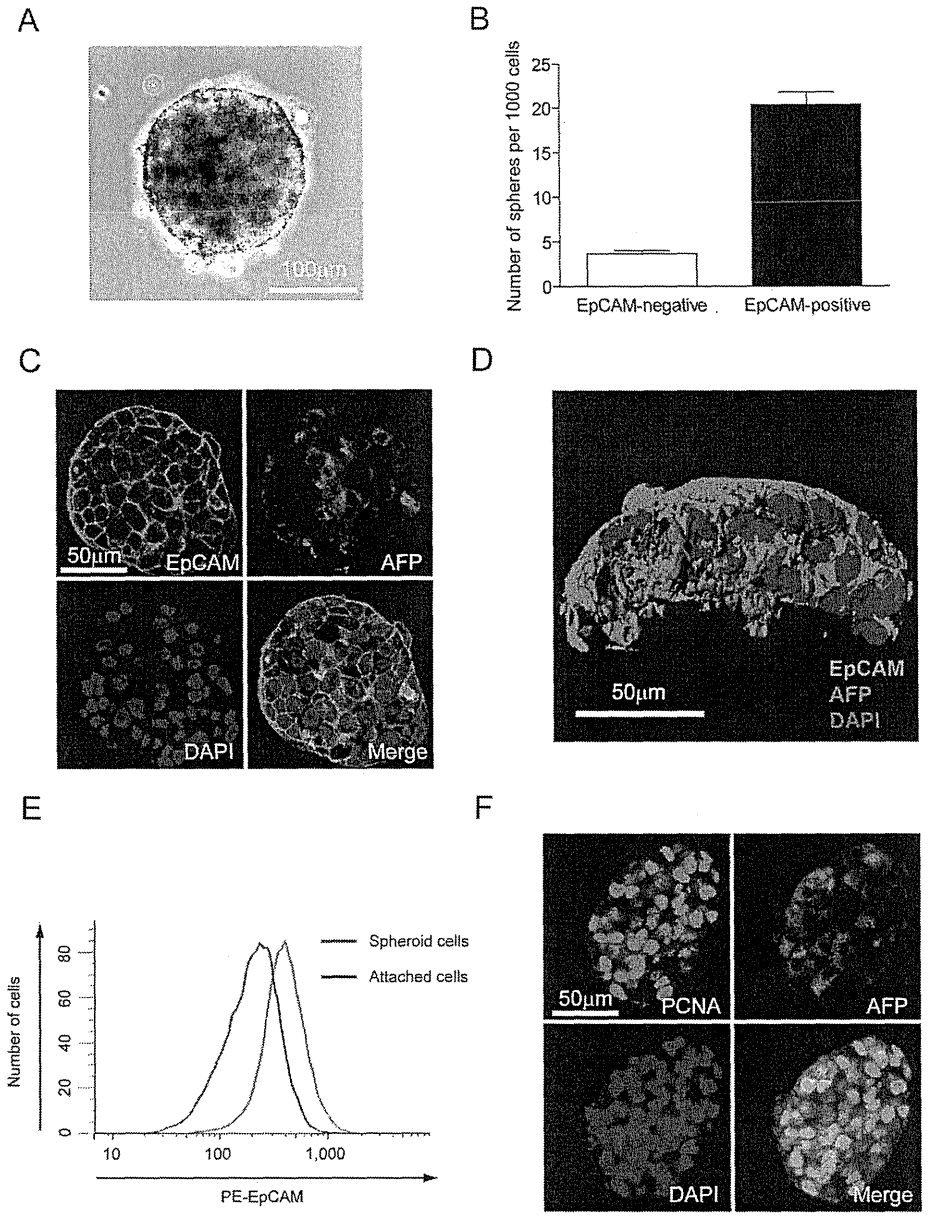

Figure 4.

Spheroid formation of EpCAM$^+$ HuH1 HCC cells. A representative phase contrast image of an HCC spheroid derived from an EpCAM$^+$ cell (scale bar = 100 μm) (A) and total numbers of spheroids from 1,000 sorted cells (B) are shown. Experiments were performed in triplicate and data are shown as mean ± SD. (C) Representative confocal images of an HCC spheroid co-stained with anti-EpCAM, anti-AFP and DAPI (scale bar = 50 μm). (D) A 3-D image of an HCC spheroid co-stained with anti-EpCAM, anti-AFP and DAPI (scale bar = 50 μm) reconstructed from confocal images using surface rendering. (E) FACS analysis of EpCAM$^+$ cells cultured as spheroids cells (red) or attached cells (blue) for 14 days after cell sorting. (F)

Confocal images of an HCC spheroid co-stained with anti-PCNA, anti-AFP and DAPI (scale bar = 50 μm).

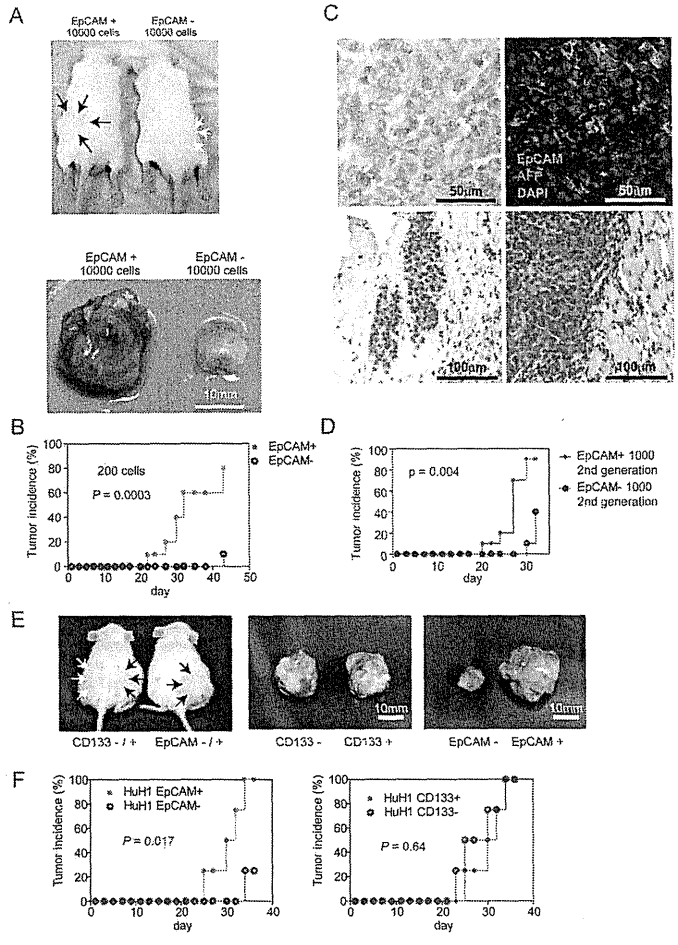

Figure 5.

Tumorigenic and invasive potential of EpCAM$^+$ HCC cells. (A) Representative NOD/SCID mice (upper panel) with subcutaneous tumors (lower panel) from EpCAM$^+$ (black arrows) or EpCAM$^-$ (white arrows) HuH1 cells. (B) Tumorigenicity of 200 sorted HuH1 cells. (C) Histological analysis of EpCAM$^+$ HuH1-derived xenografts. H&E staining of a subcutaneous tumor (left upper panel) with capsular invasion (left lower panel) and muscular invasion (right lower panel) and IF of the tumor stained with anti-EpCAM, anti-AFP, and DAPI (right upper panel) (scale bar = 50 μm). (D) Tumorigenicity of 1,000 sorted cells derived from an EpCAM$^+$ HuH1 xenograft. Data are generated from 10 mice in each group. (E) Representative NOD/SCID mice (left panel) with subcutaneous tumors from CD133$^+$ (black arrows) or CD133$^-$ (white arrows) (mid panel) and EpCAM$^+$ (black arrows) or EpCAM$^-$ (white arrows) (right panel) HuH1 cells. (F) Tumorigenicity of 1,000 HuH1 cells sorted by anti-EpCAM (left panel) or anti-CD133 (right panel) antibodies.

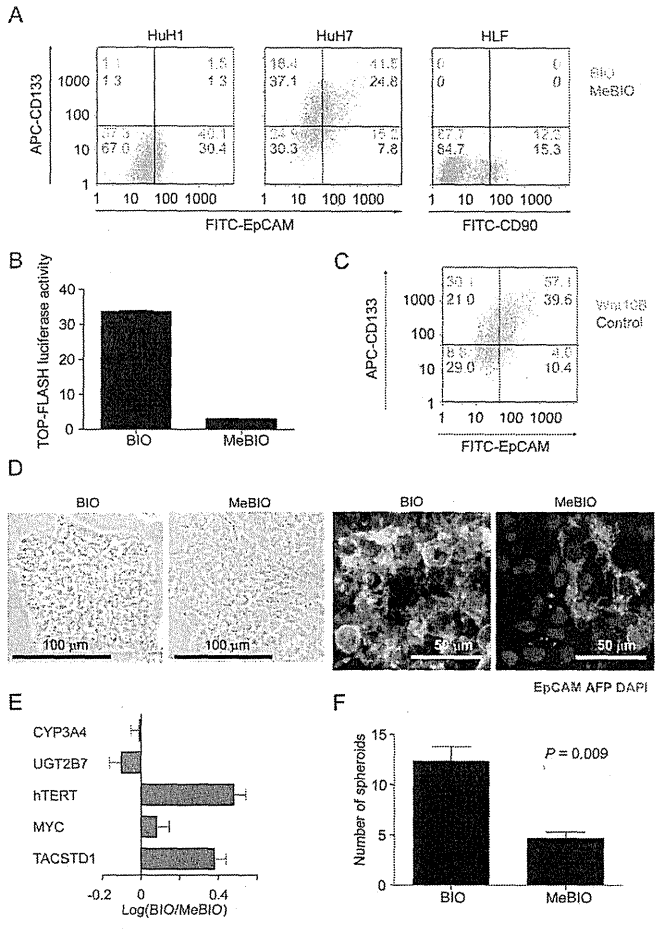

Figure 6.

Wnt/β-catenin signaling augments EpCAM$^+$ HCC cells. (A) Flow cytometer analysis of HuH1, HuH7, and HLF cells treated with 2μM of BIO (orange) or MeBIO (green) for 10 days and stained with anti-EpCAM, anti-CD133 and anti-CD90 antibodies. (B) TOP-FLASH luciferase assays of HuH7 cells treated with 2μM of BIO (red) or MeBIO (green). (C) Flow cytometer analysis of HuH7 cells cultured in the normal media (DMEM supplemented with 10% FBS) or Wnt10B conditioned media (details are described in the Materials and Methods). Cells were cultured in each medium for 2 weeks. (D) Representative phase contrast images (left panel, scale bar = 100 μm) or IF images (right panel, scale bar = 50 μm) of HuH7 cells treated with 2μM of BIO or MeBIO for 14 days. (E) qRT-PCR analysis of representative HpSC-HCC related genes in HuH7 cells treated with 2μM of BIO or MeBIO for 14 days. (F) Spheroid formation assay of HuH7 cells treated with 2μM of BIO or MeBIO for 14 days (mean ± SD).

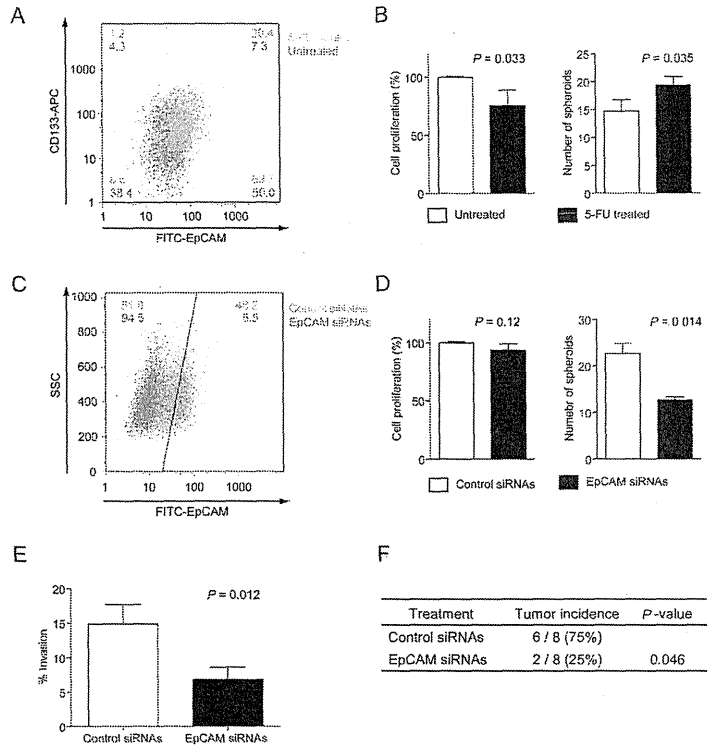

Treatment	Tumor incidence	*P*-value
Control siRNAs	6 / 8 (75%)	
EpCAM siRNAs	2 / 8 (25%)	0.046

Figure 7.

EpCAM blockage inhibits the tumorigenic and invasive capacity of EpCAM$^+$ HCC cells. (A) Enrichment of EpCAM$^+$ cells after 5-FU treatment. HuH1 cells were without (green) or treated with 2 μg/ml of 5FU for 3 days and analyzed by FACS using anti-EpCAM and anti-CD133 antibodies. (B) Spheroid formation of HuH1 cells treated with 2 μg/ml of 5FU (red) for 3 days. (C) FACS analysis of HuH1 cells treated with a control siRNA (orange) or EpCAM-specific siRNA (green) at day 3 after transfection. Spheroid formation (D) or invasive capacity (E) of EpCAM$^+$ HuH1 cells transfected with a control siRNA or EpCAM-specific siRNA. Experiments were performed in triplicate and the data are shown as mean ± SD. (F) Inhibition of tumor formation *in vivo* by EpCAM gene silencing. EpCAM$^+$ HuH1 cells were transfected with siRNA oligos and 1,000 cells were injected 24 hours after transfection.

Table 1

The tumor-initiating capacity of $EpCAM^+$ cells from clinical HCC specimens.

HCC Patients			No. of cells injected	Tumor incidence (mice with tumors/total # of mice injected)	
No.	% of $EpCAM^+$ HCC cells	Groups		2 months	3 months
1	5.2	$EpCAM^{\pm}$	1×10^3	0/3	0/3
			1×10^4	2/3	2/3
			1×10^5	2/2	2/2
		$EpCAM^-$	1×10^5	0/3	0/3
			1×10^6	0/2	0/2
2	1.4	$EpCAM^{\pm}$	1×10^3	0/2	0/2
			1×10^4	0/1	1/1
		$EpCAM^-$	1×10^4	0/3	0/3
			1×10^5	0/2	0/2

OPEN ACCESS Freely available online

PLoS one

Dicer Is Required for Maintaining Adult Pancreas

Sumiyo Morita[1,2], Akemi Hara[3], Itaru Kojima[3], Takuro Horii[1], Mika Kimura[1,2], Tadahiro Kitamura[4], Takahiro Ochiya[5], Katsumi Nakanishi[6], Ryo Matoba[6], Kenichi Matsubara[6], Izuho Hatada[1]*

1 Laboratory of Genome Science, Biosignal Genome Resource Center, Institute for Molecular and Cellular Regulation, Gunma University, Showa-machi Maebashi, Japan, **2** Japan Health Sciences Foundation, Chuo, Tokyo, Japan, **3** Department of Molecular Medicine, Institute for Molecular and Cellular Regulation, Gunma University, Showa-machi Maebashi, Japan, **4** Metabolic Signal Research Center Laboratory of Metabolic Signal, Institute for Molecular and Cellular Regulation, Gunma University, Showa-machi Maebashi, Japan, **5** National Cancer Center Research Institute, Section for Studies on Metastasis, Tsukiji, Chuo-ku, Tokyo, Japan, **6** DNA Chip Research Inc., Suehirocho, Tsurumi-ku, Yokohama, Japan

Abstract

Dicer1, an essential component of RNA interference and the microRNA pathway, has many important roles in the morphogenesis of developing tissues. *Dicer1* null mice have been reported to die at E7.5; therefore it is impossible to study its function in adult tissues. We previously reported that *Dicer1*-hypomorphic mice, whose *Dicer1* expression was reduced to 20% in all tissues, were unexpectedly viable. Here we analyzed these mice to ascertain whether the down-regulation of *Dicer1* expression has any influence on adult tissues. Interestingly, all tissues of adult (8–10 week old) *Dicer1*-hypomorphic mice were histologically normal except for the pancreas, whose development was normal at the fetal and neonatal stages; however, morphologic abnormalities in *Dicer1*-hypomorphic mice were detected after 4 weeks of age. This suggested that *Dicer1* is important for maintaining the adult pancreas.

Citation: Morita S, Hara A, Kojima I, Horii T, Kimura M, et al. (2009) Dicer Is Required for Maintaining Adult Pancreas. PLoS ONE 4(1): e4212. doi:10.1371/journal.pone.0004212

Editor: Kerby Shedden, University of Michigan, United States of America

Received October 22, 2008; **Accepted** December 9, 2008; **Published** January 16, 2009

Funding: This work was supported in part by the Japan Health Sciences Foundation (S.M. is a fellowship holder from the Japan Health Sciences Foundation), grants from the Ministry of Education, Culture, Sports, Science and Technology of Japan (I.H. and I.K.), the Ministry of Health, Japan Health Sciences Foundation, Labor and Welfare of Japan (T.O. and I.H.) and a grant from the Realization of Regenerative Medicine (I.K.). The funders had no role in study design, data collection and analysis, decision to publish, or preparation of the manuscript.

Competing Interests: The authors have declared that no competing interests exist.

* E-mail: ihatada@showa.gunma-u.ac.jp

Introduction

MicroRNA (miRNA) is small (~22 nucleotides), non-coding RNA. Mature miRNA transcribed as long primary transcripts is processed to pre-miRNA in the nucleus by *Drosha/DGC8* [1], and then processed in the cytoplasm by *Dicer* [2]. MiRNA is further incorporated into the RNA-inducing silencing complex (RISC), which includes Argonaute [3] to regulate gene expression via post-transcriptional repression. Over the past few years, more than 400 miRNAs have been identified, but their function is largely unknown. Several miRNAs exhibit tissue-specific or developmental stage-specific expression [4,5], indicating that they have important roles in many biological processes.

Dicer1 encodes an RNaseIII endonuclease, a key enzyme that processes miRNA. It is broadly expressed in developing tissues, and several mutant alleles of *Dicer1* have been generated in mice. *Dicer1* seems to be critical in early development since loss of its function was lethal at embryonic day 7.5 [6]. Characterization of *Dicer1* hypomorphic mice showed that the gene is required for embryonic angiogenesis [7]. Conditional inactivation of *Dicer1* in the mouse limb bud mesenchyme [8], lung epithelium [9], epidermal hair follicle [10], and pancreas [11], T cell development and differentiation [12] led to the conclusion that *Dicer1*, which processes miRNA, is indispensable for the development and morphogenesis of these tissues.

We previously generated *Dicer1*-hypomorphic mice (homozygous *Dicer1*−/− mice) [13]. Complete loss of *Dicer1* in mice results in early embryonic death [6]; however, our *Dicer1*-hypomorphic mice were viable [13]. To study the function of *Dicer1* in the maintenance of homeostasis in adult tissues, we analyzed the adult tissues histologically and found abnormalities only in the pancreas. The phenotypes detected in the pancreas of *Dicer1*-hypomorphic mice might resemble the differentiation of endocrine precursor cells in adult pancreas.

The pancreas consists of three main tissue cell types: the endocrine cells (islet of Langerhans) which produce hormones such as insulin and glucagon; the exocrine acinar tissues which secrete digestive enzymes; and the branched duct. Numerous mechanisms that control the differentiation of endocrine and exocrine cells in the embryonic pancreas have been revealed [14], but how endocrine cells (especially insulin-producing β cells) are maintained in postnatal life has been controversial [15]. At E9.5, the endocrine cells of the pancreas arise from endocrine precursor cells, which express both glucagon and insulin and divide into distinct lineages such as glucagon or insulin-expressing cells. On the other hand, in the adult pancreas, it had been considered that there are no endocrine progenitor cells and that β cells are generated only by the replication of existing β cells, not from the differentiation of endocrine precursor cells (neogenesis) [16,17]. However, several studies suggested that β cell differentiation from endocrine precursor cells can occur in adults in the regenerating pancreas after a partial pancreatectomy or duct ligation [18,19,20,21]. In the regenerating pancreas, vigorous expansion of the β cell population was observed, and partial pancreatectomy and duct ligation has been a good model for regenerating endocrine cells. The phenotypes observed in *Dicer1*-hypomorphic

mice suggested that *Dicer1* regulates the endocrinal neogenesis in the adult pancreas. Previous study showed that *Dicer1* is indispensable for normal development of the pancreas [11]; however, its function in the adult pancreas had not been elucidated. Here we report that *Dicer1* also has important functions in the adult pancreas.

Results

Dicer1 expression was significantly reduced in all tissues of *Dicer1*-hypomorphic mice but histological abnormalities were only found in the pancreas

Dicer1-hypomophic mice (homozygous *Dicer1*−/− mice) showed a lower birth rate than expected by Mendelian rules [13]; however, they did not differ from their wild-type littermates in overall health. Although they showed slight growth retardation from 10 to 50 days of age, their body weight was similar to that of wild-type mice after 50 days of age (Fig. 1). A comparison of *Dicer1* expression in nine tissues of adult mice revealed a 70–85% reduction in the hypomorphic mice (Fig. 2). Although we analyzed more than 40 tissues (Table 1), histological examination revealed no abnormalities in any tissues except the pancreas (Fig. 3); thus we focused on the pancreas of *Dicer1*-hypomorphic mice.

Dicer1 could be involved in differentiation of endocrine cells in adult pancreas

In *Dicer1*-hypomorphic mice, the size of the pancreas in adults (8–10 weeks of age) was nearly identical to that in the wild-type mice; however, there were more small islets (Fig. 4). In some of these islets, the distribution of islet cells and staining of nuclei were irregular (Fig. 5A). The boundary of islets and ducts was not clearly defined in the pancreas (Fig. 5B). Immunohistochemical analysis revealed mostly normal staining of insulin and glucagon at 8–10 weeks of age; however, the number of ductal epithelial cells stained with insulin or glucagon was significantly increased (Fig. 5C-III, P = 0.0051). In some models of pancreatic regeneration including partial pancreatectomy, insulin or glucagon-stained cells are present in the ductal epithelium, which had led to the idea that some endocrine cells differentiate in the ducts [18,19,20,21]. Our observations in *Dicer1*-hypomorphic mice suggest that regeneration from the endocrine precursor cells took

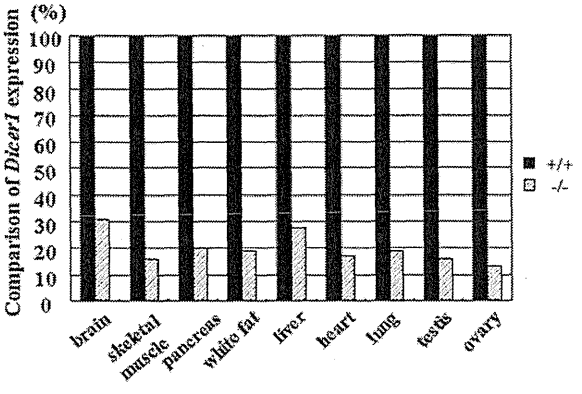

Figure 2. Comparison of *Dicer1* expression in nine tissues between wild-type (+/+) and *Dicer1*-hypomorphic (−/−) mice. The expression in the *Dicer1*-hypomorphic mice was normalized to that in the wild-type mice.
doi:10.1371/journal.pone.0004212.g002

place in adulthood. Next we conducted a histological examination of the markers Pdx-1 and Ki67. The population of ducts containing Pdx-1-positive cells was significantly increased (Fig. 5C-IV, P = 0.009). Pdx1-positive cells in the ducts are possibly the adult progenitor cells [22,23], and PDX-1 protein was detected in the pancreatic duct in adult rats after partial pancreatechtomy [21]. Surprisingly, abnormal staining of Ki67, which is a marker for proliferation of the cells, was detected in the pancreatic ducts in two of six *Dicer1*-hypomorphic mice (Fig. 5C-V). In some Ki-67-positive ducts, all the epithelial cells were stained. No such observations were found in wild-type mice.

Interestingly, cells morphologically different from either acinar or islet cells were observed in *Dicer1*-hypomorphic mice (Fig. 5D-I). Under a light microscope, some appeared to be syncytial multinucleated cells near the pancreatic duct and in acini. Numerous nuclei were distributed irregularly and were often clustered in the cells, which were all double-positive for insulin and glucagon (Fig. 5E). Cells double-positive for insulin and glucagon were significantly increased in *Dicer1*-hypomorphic mice compared to wild-type mice (Fig. 5D-II, P = 0.0019). In the exocrine portion of

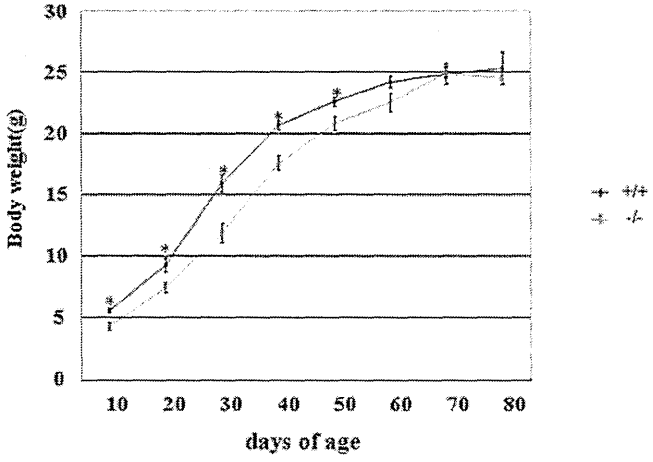

Figure 1. Body weight growth curves. Male wild-type (+/+) and *Dicer1*-hypomorphic (−/−) mice were measured to determine the change in body weight from 10 to 80 days of age. *, P<0.05. n = 8–10 per group.
doi:10.1371/journal.pone.0004212.g001

Table 1. The list of tissues with histological analysis (H&E assessment).

lung	testis	eye boll	trachea
heart	epididymis	harderian gland	esophagus
kidney	prostate	skeletal muscle	thyroid gland
pancreas	seminal vesicle	sciatic nerve	liver
tongue	coagulating gland	skin	cholecyst
stomach	bladder	breast bone	spleen
duodenum	adrenal	femur	
jejunum	pituitary gland	cerebrum	
ileum	submandibular gland	hippocampus	
cecum	parotid gland	thalamus	
colon	thymus	cerebellum	
rectum	cervical lymph node	spinal cord	

Histological analysis of these tissues was performed in wild-type (+/+) (n = 2) and *Dicer1*-hypomorphic (−/−) mice (n = 4).
doi:10.1371/journal.pone.0004212.t001

the pancreas of *Dicer1*-hypomorphic mice, most acini were morphologically normal, but some showed an irregular morphology (Fig. 5F). The shapes and position of the cells were irregular and the acinar structure was not organized. In normal acinar cells, zymogen granules are observed in the center of the acinus and the nucleus is located at its periphery.

We next investigated when the abnormal morphology appeared in the development of the pancreas in *Dicer1*-hypomorphic mice. For this purpose, a histological analysis was performed using E15.5 embryos, P1 mice, and 4-week-old mice. The pancreas of both wild-type and *Dicer1*-hypomorphic mice developed normally and endocrine and exocrine cells appeared morphologically normal at E15.5 and P1 (Fig. 6A, B); the same abnormalities observed in adult *Dicer1*-hypomorphic mice were detectable at 4 weeks of ages (Fig. 6C), although the number of abnormal cells was less than that found in adult *Dicer1*-hypomorphic mice. This suggested that the pancreas of *Dicer1*-hypomorphic mice developed normally after birth and abnormal cells appeared at around 4 weeks after birth, increasing with age.

Surprisingly, the observations found in *Dicer1*-hypomorphic mice were quite similar to the histological findings in transgenic mice expressing a truncated type II activin receptor [24]. Therefore, we next investigated the expression of the activin type II receptor in the pancreas of *Dicer1*-hypomorphic mice. Two related receptors, ActRIIA and ActRIIB, were initially identified as type II receptors for activin [25,26]. ActRIIA and ActRIIB have been reported to bind not only to activin [27], but also to other TGF-β family proteins, including BMP7 [28], GDF8 [29], Nodal [30], and GDF11 [31]. The precise role of the two activin receptors is still not clear. Real-time PCR analysis revealed that the expression of ActRIIA was slightly up-regulated in *Dicer1*-hypomorphic mice compared to wild-type mice, while the expression of ActRIIB did not differ (Fig. 7). Therefore, the abnormal morphology might be attributed to another signaling cascade.

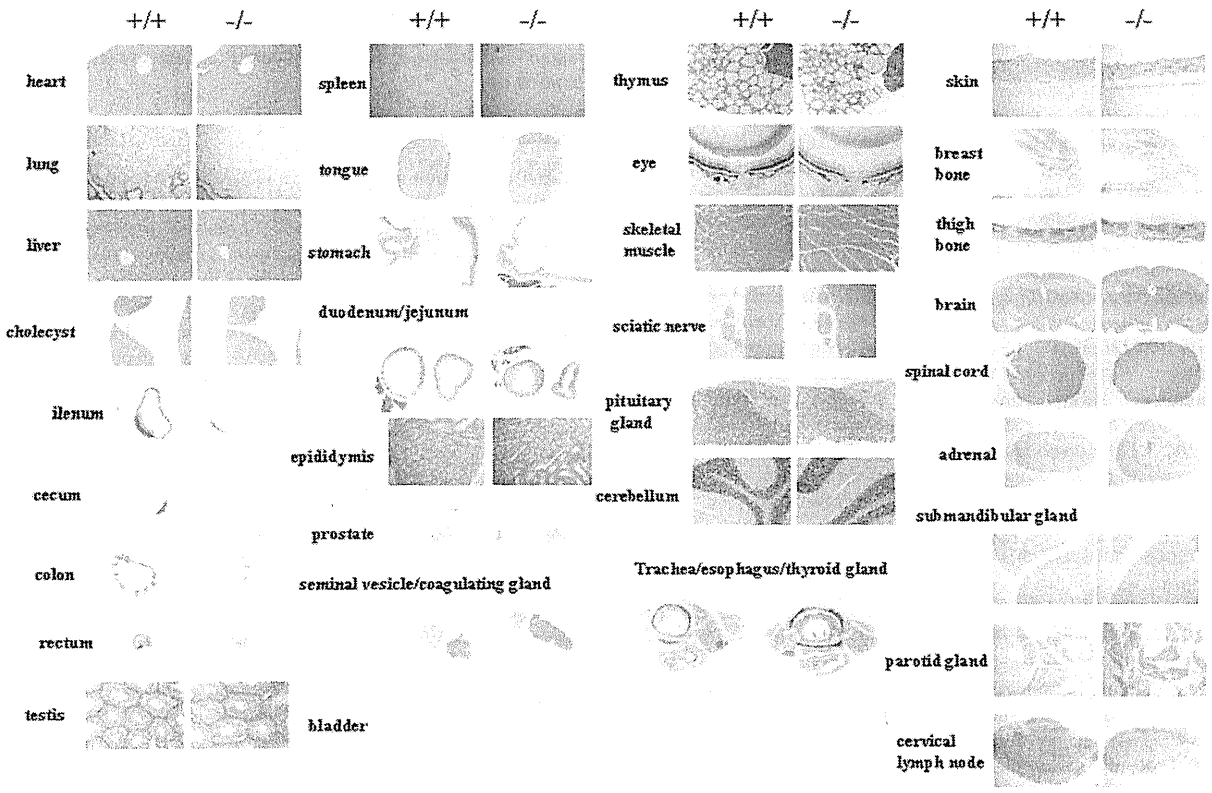

Figure 3. H&E-stained section of adult tissues of wild-type (+/+) (n = 2) and *Dicer1*-hypomorphic (−/−) mice (n = 4).
doi:10.1371/journal.pone.0004212.g003

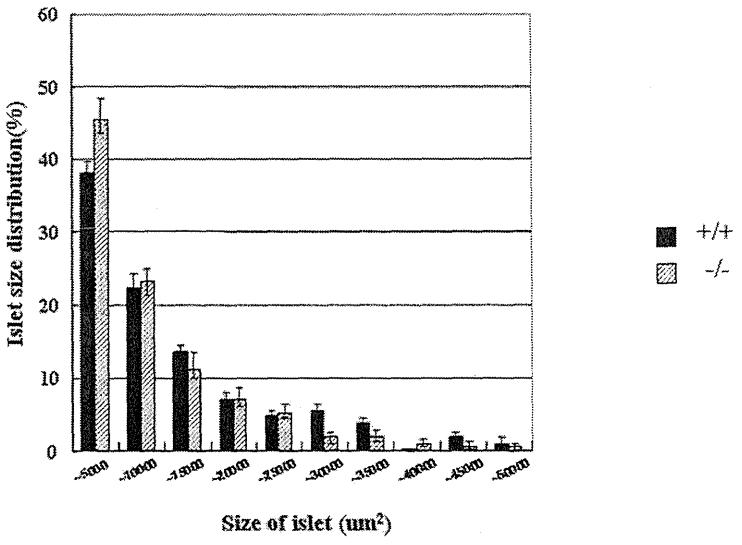

Figure 4. Comparison of the size of islets in wild-type and *Dicer1*-hypomorphic mice. The islets mass was measured in wild-type (blue bar) and *Dicer1*-hypomorphic mice (pink bar). The numbers of islets were examined in wild-type (n = 6) and *Dicer1*-hypomorphic (n = 6) mice, with six sections from each animal. The graph shows the percentage of islets in each size category.
doi:10.1371/journal.pone.0004212.g004

Detection of differential expressed miRNAs by microarray analysis

Because *Dicer1* is required for the processing of miRNAs, the reduction of *Dicer1* results in a decrease in miRNAs. To determine the differential expression of miRNAs in the pancreas of adult wild-type and *Dicer1*-hypomorphic mice, a miRNA microarray analysis was performed. The miRNAs of the pancreas of two wild-type and two *Dicer1*-hypomorphic mice were analyzed. Signals were very weak on hybridization with miRNA in the pancreas compared to other tissues; therefore a total of 83 miRNAs, which showed strong signals, were analyzed. Fig. 8 shows the change in the distribution of miRNA levels in *Dicer1*-hypomorphic mice compared to wild-type mice. Surprisingly, miRNA expression did not dramatically change in *Dicer1*-hypomorphic mice compared to the wild-type animals: however, 7% of miRNAs were down-regulated less than 0.5 fold. These miRNAs might function in maintaining the adult pancreas, but at present their relationship with the abnormal phenotype in *Dicer1*-hypomorphic mice is unclear. Why was only 7% of the miRNA expressed in pancreas attenuated? Dicer1 protein might catalyze processing of pre-miRNA differently dependent on the sequence when generating miRNA. The down-regulated miRNAs might be more difficult to process than the other miRNAs and thus significantly reduced *Dicer1* expression might affect their generation.

Glucose metabolism was normal in *Dicer1*-hypomorphic mice

The hypo-expression of *Dicer1* leads to abnormal endocrine cells, which might affect the function of the pancreas; therefore, we next investigated the metabolism of glucose in *Dicer1*-hypomorphic mice. Despite histological abnormalities in pancreatic islets, a glucose tolerance test showed that *Dicer1*-hypomorphic mice were able to clear glucose from the blood as efficiently as wild-type mice (Fig. 9A), and had insulin levels similar to wild-type mice (Fig. 9B). Despite no significant differences in the insulin content of serum after overnight fasting, *Dicer1*-hypomorphic mice showed a slightly reduced blood glucose level on fasting. *Dicer1*-hypomorphic mice were smaller than the wild-type mice before 50 days of age; therefore, we hypothesized that the growth hormone level affects fasting hypoglycemia. We checked the blood growth hormone level; however, we found no significant differences with wild-type mice (Fig. 9C). Thus, the growth hormone level is not responsible for fasting hypoglycemia in *Dicer1*-hypomorphic mice, probably due to an unknown mechanism involved in glucose metabolism in other tissues.

Discussion

Dicer, the enzyme that generates miRNAs, has been reported to have quite important roles in a variety of developmental processes. In our *Dicer1*-hypomorphic mice, histological analysis (H&E assessment) showed that the abnormalities were found only in the pancreas and not in other tissues. However, we could not exclude the possibility that there are more minute structural abnormalities not detected with the H&E assessment, or functional abnormlities. In this study, we focused on the pancreas. The pancreatic-specific knockout of *Dicer1* clarified that miRNA is required for the development of the pancreas in embryogenesis [11]. Our study suggested that *Dicer1* also has important functions in maintaining the adult pancreas.

Histological abnormalities such as the irregular distribution of islet cells, and deviations from the typical structure of the acinus, were found in endocrine and exocrine cells in the adult pancreas of *Dicer1*-hypomorphic mice, although none of these abnormalities were detected before 4 weeks of age. *Dicer1* is indispensable for normal pancreatic cell differentiation at embryogenesis [11]. The pancreas-specific *Dicer1* knockout mice survived until birth but died before P3. These mice showed gross defects in all pancreatic lineages, and the formation of exocrine cells and duct cells, especially endocrine cells, was greatly impaired. Given that miRNA most probably plays essential roles in the morphogenesis of many tissues in a developing embryo [7,8,9,10,12], the gross defects in all pancreatic lineages observed upon removal of *Dicer1* are not surprising. These mice died soon after birth; therefore, it is impossible to study the role *Dicer* may play in adult tissues.

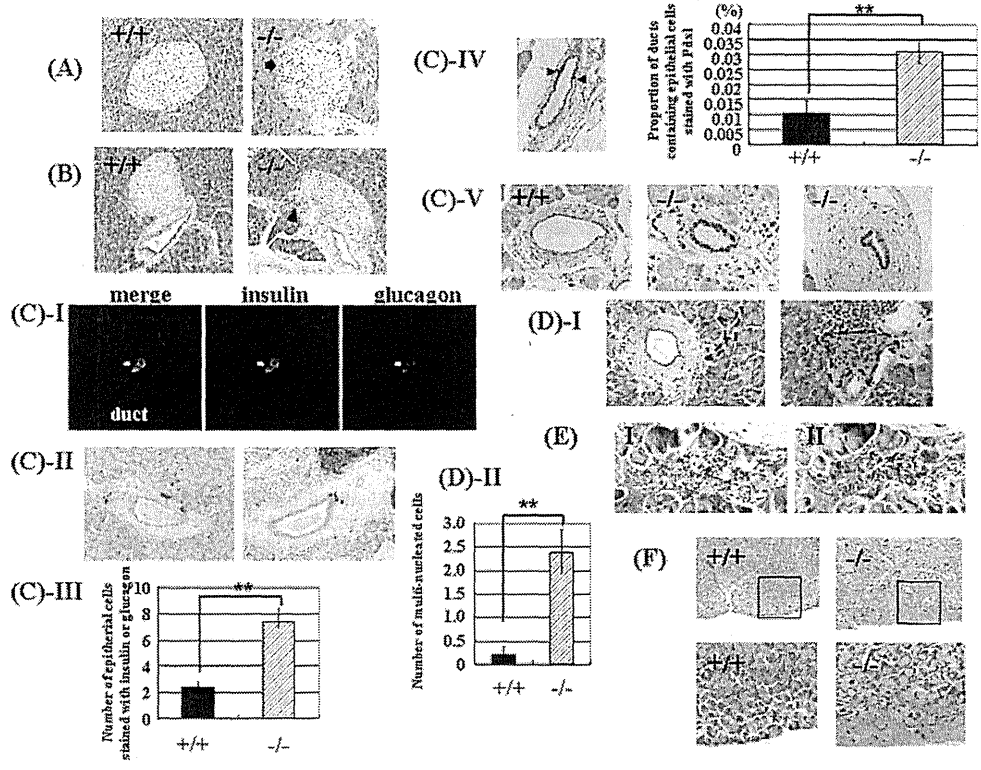

Figure 5. Pancreas morphology in adult (8–10 weeks of age) *Dicer1*-hypomorphic mice. A, B: Hematoxylin-eosin (H & E)-stained islets of the pancreas from an 8-week-old wild-type (+/+) mouse and *Dicer1*-hypomorphic (−/−) mice (*400). A: Arrows indicate an irregular distribution of islet cells. B: Arrowheads indicate that the boundary of islets and ducts was not clearly defined in the pancreas of *Dicer1*-hypomorphic mice. C: Immunohistochemistry of duct cells of *Dicer1*-hypomorphic mice. (I) Insulin (green) and glucagon (red) double-expressing cells were detected in the duct. (II) Insulin-positive cells (brown) and glucagon-positive cells (blue) were observed in the duct. (III) Comparison of the number of epithelial cells stained with both insulin and glucagon, only insulin, and only glucagon in wild-type and *Dicer1*-hypomorphic mice. These numbers were averaged from 6 animals, with six sections from each animal. **, $P<0.01$. (IV) Comparison of the proportion of ducts containing epithelial cells stained with Pdx1 in wild-type and *Dicer1*-hypomorphic mice. Arrowheads indicate the Pdx1-positive cells. *, $P<0.01$. (V) Abnormal staining of Ki67 was observed in the pancreas of *Dicer1*-hypomorphic mice. D: (I) H & E-stained multinuclear atypical cells in the pancreas of *Dicer1*-hypomorphic mice. The black dotted line indicates atypical multinuclear cells. (II) Comparison of the number of multi-nucleated cells in wild-type and *Dicer1*-hypomorphic mice. These numbers were averaged from 6 animals, with six sections from each animal. **, $P<0.01$. E: Immunohistochemistry of multinuclear atypical cells of adjacent sections of the pancreas of *Dicer1*-hypomorphic mice using anti-insulin (I) and anti-glucagon (II) antibodies. F: H & E-stained acinar cells. The rectangular areas outlined in the upper panels are magnified in the lower panels. An abnormal structure of exocrine cells was observed in the pancreas of *Dicer1*-hypomorphic mice.

doi:10.1371/journal.pone.0004212.g005

The pancreas of our *Dicer1*-hypomorphic mice developed normally and the reduced expression of *Dicer1* did not affect the development of the pancreas during embryogenesis or the neonatal stage. However, aberrant endocrine and exocrine cells could be detected after 4 weeks of age, and the number of abnormal regions seemed to increase with age. It is interesting that the developing pancreas during embryogenesis and the adult pancreas differ in sensitivity to the *Dicer1* level. In other words, the reduction in *Dicer1* only affects the maintaining of adult pancreas, not the normal development of the pancreas.

In addition, these observations, such as the increasing number of ductal epithelial cells stained positive for insulin, glucagon, and Pdx-1 in *Dicer1*-hypomorphic mice (Fig. 5D-III, IV), were also found in the regenerating pancreas [18,19,20,21], suggesting that the differentiation of endocrine precursor cells (neogenesis) occurred in the adult pancreas. Moreover, a quite intriguing observation was the existence of unknown abnormal multi-nucleated cells in the pancreas that expressed both glucagon and insulin. In the developing pancreas, endocrine precursor cells first appeared at E9, and these cells expressed both glucagon and insulin [32,33], then differentiated into insulin-producing cells or glucagon-producing cells. These cells in our adult *Dicer1*-hypomorphic mice resembled endocrine precursor cells in the fetal pancreas in terms of the expression of both glucagon and insulin. Therefore, *Dicer1* might have roles in regulating endocrine precursor cells in the adult pancreas.

The proliferation of duct cells is increased in the regenerating pancreas compared to the normal adult pancreas [20]. However, in some *Dicer1*-hypomorphic mice, abnormal proliferation of duct epithelial cells was observed (Fig. 5D-V). These features were not detected in wild-type mice and could be caused by the reduction in *Dicer1*.

Surprisingly, these histological observations in *Dicer1*-hypomorphic mice were quite similar to the histological findings in transgenic mice expressing the truncated type II activin receptor [24]. However, as our *Dicer1*-hypomorphic mice showed only a 1.2-fold increase in ActRIIA in the pancreas, ActRIIA might not cause the abnormal phenotype.

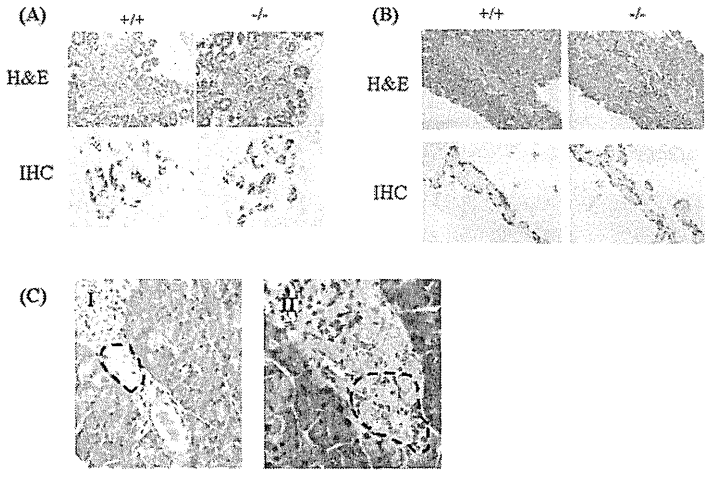

Figure 6. Histological and immunohistochemical analysis of the pancreas at E15.5 (A) and P1 (B) of wild-type and *Dicer1*-hypomorphic mice. *Dicer1*-hypomorphic mice show normal insulin (brown) and glucagon (blue) staining at E15.5 and P1. C: Histological abnormalities found in the pancreas of 4-week-old *Dicer1*-hypomorphic mice. (I) The endocrinal distribution was slightly irregular. The dotted line indicates the abnormal region of the islet. (II) Multi-nucleated cells were observed. The dotted line indicates multi-nucleated cells, which were also found in the pancreas of adult *Dicer1*-hypomorphic mice.
doi:10.1371/journal.pone.0004212.g006

Because *Dicer1* has a key role in generating a large number of miRNAs, its removal results in a significant decrease in miRNAs. In the pancreas of our *Dicer1*-hypomorphic mice, the expression levels of miRNA changed slightly compared to wild-type level which is why the mice could survive. A complete loss of *Dicer* in mice results in early embryonic death. A large number of genes control the development or maintenance of the pancreas, and these genes might be a potential target of miRNAs. Even a slight change in miRNA expression might affect the gene expression, leading to the abnormal morphology in *Dicer1*-hypomorphic mice. Further exploration is necessary to investigate the relation between these genes and miRNA in the pancreas.

Our results suggest that *Dicer1* functions in the adult pancreas and also raise the possibility that *Dicer1* regulates the differentiation of endocrine precursor cells there. Further analysis is necessary to understand the mechanism behind the maintenance of each cell type in the adult pancreas, especially β cells.

Materials and Methods

Gene targeting and mice

We generated *Dicer1*-deficient mice from an ES cell (RFF266), which was obtained from Bay Genomics [34], carrying a gene trap insertion between exon 22 and exon 23, resulting in disruption of the second RNaseIII domain and loss of the double-stranded RNA-binding domain. A gene trap vector called pGT1Lxf, which has a splicing acceptor, was used to make this ES cell. Targeted clones were injected into blastocysts to generate chimeras. Five chimeras were generated and backcrossed with

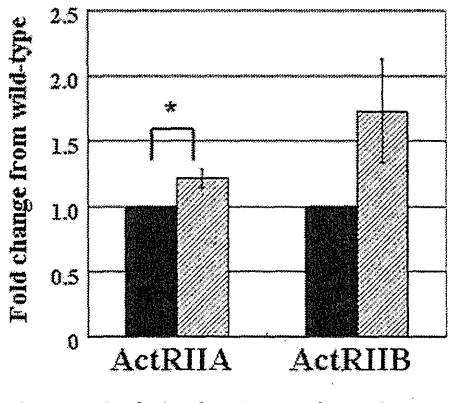

Figure 7. Analysis of ActRIIA and ActRIIB expression. Data are expressed relative (n-fold) to the wild-type pancreas and correspond to the means and standard errors for three independent experiments performed in triplicate. *, $P<0.05$. wild-type n = 9, *Dicer1*-hypomorphic mice n = 9.
doi:10.1371/journal.pone.0004212.g007

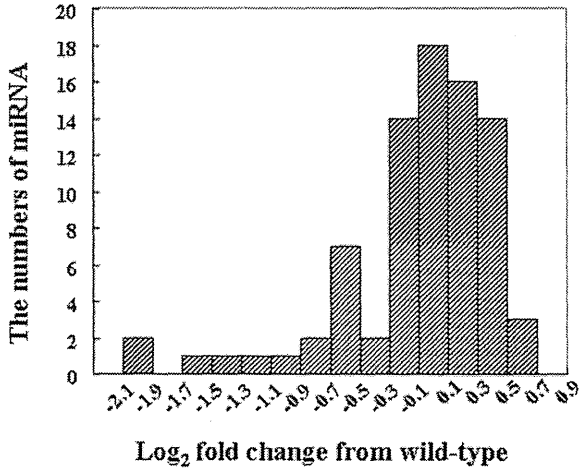

Figure 8. The distribution of changes in miRNA levels in *Dicer1*-hypomorphic mice compared to wild-type mice.
doi:10.1371/journal.pone.0004212.g008